Received: 4 March 2023 | Accepted: 12 April 2024

DOI: 10.1002/rmb2.12578

Reproductive Medicine and Biology

WILEY

REVIEW

Morphokinetic features in human embryos: Analysis by our original high-resolution time-lapse cinematography—Summary of the past two decades

Yasuyuki Mio | Keitaro Yumoto | Minako Sugishima | Minori Nakaoka | Toko Shimura | Panagiota Tsounapi

Reproductive Centre, Mio Fertility Clinic, Yonago, Japan

Correspondence
Yasuyuki Mio, Reproductive Centre, Mio Fertility Clinic, 2-1-1, Kuzumo-Minami, Yonago 683-0008, Japan.
Email: yasmio@mfc.or.jp

Abstract

Background: The pioneering work by Dr. Payne et al. in time-lapse cinematography for observation of the morphokinetic features of human embryos inspired us to develop a new in vitro culture system with high-resolution time-lapse cinematography (hR-TLC) back in 2001.

Methods: This in vitro culture system was capable of maintaining stable culture and was constructed on an inverted microscope stage. Embryos were observed and photographed noninvasively for an extended period, up to 7 days. The obtained images were displayed at a speed of 30 frames per second and individually analyzed.

Results: Using hR-TLC, human fertilization and subsequent embryonic development were visualized, revealing the time course of phenomena and many unusual dynamics.

Conclusion: In this review, we summarize the results of our hR-TLC analysis of early human embryonic development over the past 20 years. In the near future, it is expected that the vast amount of information obtained by hR-TLC will be integrated into the AI system for further analysis and to provide feedback that will have the potential to improve clinical practice. In the era of SDGs and environmental awareness, we should be cautious about the direction in which AI can be utilized to avoid any further harm to the planet.

KEYWORDS
embryo development, embryo early cleavage, fragmentation, morphokinetic evaluation, time-lapse cinematography

1 | INTRODUCTION

Since the advent of human-assisted reproductive technologies (ART) in 1978, we have had the opportunity to catch a glimpse of conception and the subsequent period, through microscopic fixed-point observations. However, there were inevitable limitations in the detailed analysis of human embryonic development using still images during an in vitro culture system. In 1997, D. Payne et al. developed a time-lapse video cinematography (TLC) system for dynamic analysis of early human embryonic development. The authors observed human oocytes by TLC for 17–20 h after intracytoplasmic sperm injection (ICSI) and found several novel and impressive features.[1] However, in that

study, the observation time by TLC was limited to 17–20 h. Therefore, we came up with the idea that if an in vitro environment on the stage of an inverted microscope could be maintained as optimal and stable as that of a conventional incubator for an extended period of time, the previously unknown process of human embryo development from fertilization and beyond could be analyzed in more detail.

Therefore, in 2001, we began to develop an in vitro culture system that could maintain a stable culture environment for human embryos on the stage of an inverted microscope for a long period of time. Eventually, two years later, we were able to complete the development of an in vitro culture system for TLC (high-resolution time-lapse cinematography; hR-TLC). Using the in vitro culture system for hR-TLC, we have been analyzing detailed hR-TLC images of human oocytes from fertilization to the blastocyst stage before implantation for 20 years. For the first time, we have been able to visualize various phenomena related to the birth of life that were previously unknown.[2–5] In this review article, we present a compilation of numerous human embryo behaviors that we have obtained from the hR-TLC analysis, and we had the privilege to observe for the first time using our hR-TLC in vitro culture system.

2 | METHODS

2.1 | Development of an in vitro culture system for hR-TLC

Initially, we attempted to prepare a system similar to the one developed by D. Payne et al. However, it was difficult to maintain optimal conditions (temperature: 37.0 ± 0.5°C, pH: 7.37 ± 0.2) for the culture medium for a long time in the system. Therefore, we decided to originally develop a new culture system where the culture medium can be maintained in an optimal environment on the stage of an inverted microscope and, at the same time, high-resolution images of embryos can be captured.

2.1.1 | Original concept of the in vitro culture system

For a stable culture environment, it is essential to maintain optimal temperature and pH levels. For this purpose, the inverted microscope was entirely covered with a large acrylic resin chamber with multiple operating windows, and a small acrylic resin chamber (15 cm × 15 cm × 3 cm) was placed on the microscope stage for embryo culture. The dedicated small chamber had a space (40 mm diameter) in the center for placing embryo culture dishes, and the chamber was surrounded by a water bath. To maintain the culture medium in the embryo culture dishes at the optimal temperature (37.0 ± 0.5°C), a heating device (Kohken Engineering, Saitama, Japan) was placed inside the large chamber, and a thermo-plate (Tokai Hitachi, Shizuoka, Japan) was used on the stage of the microscope. The water bath, which was filled with pure water (Milli-Q, Merck Millipore, USA) and infused with medical carbon dioxide gas (CO_2), functioned to stabilize the temperature and to maintain the optimal pH (7.37 ± 0.2) in the culture medium (Figure 1). In this device, it was necessary to set the temperature of the heating device at 37°C and the thermoplate at 38°C to maintain the temperature in the culture medium at 37°C. In addition, to maintain the optimal pH of the culture medium, 40 mL/min of CO_2 was required to flow into the central space after heating and humidifying through the water bath. The culture medium was always covered with mineral oil (Sage, Pasadena, CA) to stabilize optimal culture conditions for a long period of time. Furthermore, the in vitro culture system was entirely covered with light-shielding cloth during the culture and observation of human embryos.

2.1.2 | Acquisition of high-resolution images

To obtain high-resolution tomographic images, the inverted microscope (IX-70, Olympus Optical Industries, Tokyo, Japan) was equipped with a Nomarski differential interference contrast (DIC) device (Olympus Optical Industries, Tokyo, Japan). Since a plastic dish was not suitable for using the DIC device to obtain high-resolution images, we always used a glass-bottom dish (FluoroDishTM, World Precision Instruments. Inc., FL, USA) when culturing and taking photographs of embryos.

2.1.3 | Continuous observation and photography using hR-TLC and imaging of human embryos

For continuous observation and photography of embryos cultured in a small chamber, a CCD digital camera (Roper Scientific Photometrics,

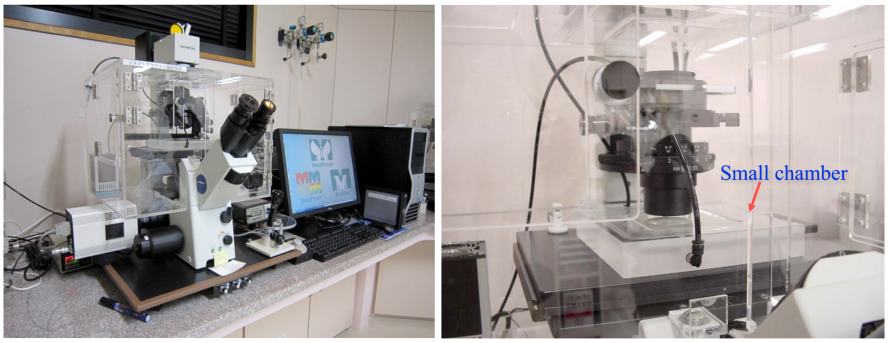

FIGURE 1 The original in vitro culture system for high-resolution time-lapse cinematography developed by our clinic. Culture conditions of the bottom of the small medium drop in the culture dish placed in the small chamber. Temperature: 37.0 ± 0.5°C, pH: 7.37 ± 0.02.

Tucson, AZ) was attached to an inverted microscope, and the images captured were accumulated on a connected computer. Image acquisition conditions were controlled using MetaMorph (Universal Imaging Co, Downingtown, PA). The exposure time for image acquisition was set at 50 μsec, and although the interval of photography between images could be set arbitrarily, the interval was set at 10 s until the sperm penetrated the zona pellucida (ZP) and incorporated into the ooplasm, and at 2 min intervals thereafter. During early hR-TLC observation, 2000–2500 images were taken because of the computer capacity. Therefore, the maximum period of observation was approximately 40 h. Subsequently, the image storage capacity increased dramatically, enabling the storage of more than 8000 images and up to 7 days of embryo development observation imaging. The obtained images were reproduced and displayed at 30 frames per second.

2.2 | Preparation and subsequent procedure of oocytes/embryos submitted for hR-TLC

2.2.1 | Embryos for therapeutic purposes

In patients with conventional in vitro fertilization (cIVF) or intracytoplasmic sperm injection (ICSI), according to medical indications, oocyte retrieval was performed under transvaginal ultrasound guidance after controlled ovarian stimulation with GnRH analogues.

In patients with cIVF, collected oocytes were inseminated with 50 000 motile spermatozoa according to our protocol.[6] Among the patients who gave consent for hR-TLC analysis, one inseminated oocyte was randomly selected from the patients who had multiple oocytes and submitted to the hR-TLC observation. At 1 h after insemination, the cumulus cells surrounding the selected oocyte were mechanically removed to avoid damaging sperm tails, and they were transferred into a medium drop (20 μL) in the glass-bottom dish for observation and photography. The sperm penetration site of the ZP was carefully identified using a micromanipulator (Narishige Co., Tokyo, Japan) attached to an injection needle (TZP-LCS, TPC, Adelaide, Australia) used for ICSI. After distinguishing the sperm that had penetrated most deeply into the ZP, we focused the microscope on the sperm and commenced hR-TLC observation for approximately 40 h. However, it was extremely challenging to predict which sperm would penetrate the ZP. The remaining sibling oocytes were cultured in a bench-top incubator (MINC, Cook Co., Brisbane, Australia) following the routine IVF procedure. After the hR-TLC observation, embryos developed to good quality based on Veeck's criteria modified according to the Istanbul Consensus and were cryopreserved for subsequent clinical use.[7,8]

In patients with the ICSI procedure, the cumulus cells of the oocytes collected were gently removed approximately 1 h after oocyte retrieval. Denuded oocytes (Metaphase II; MII) were precultured for at least 3 h and ICSI was performed on the oocytes according to the method previously described.[9–11] In the patients with multiple oocytes who consented to participate in this study, one of the oocytes was randomly selected and was immediately transferred to a medium drop in the in vitro culture system for hR-TLC. The remaining sibling oocytes were cultured in a bench-top incubator. Embryos with good quality on day 2 were cryopreserved for future clinical use.

2.2.2 | Embryos for research purposes

Cryopreserved embryos that were not planned to be used for future clinical treatment and the couples had decided to donate them for research were used for hR-TLC observation. In this way, we had the opportunity to examine the effects of prolonged culture on embryonic development. By this procedure, we managed to make the necessary modifications, optimize our hR-TLC in vitro culture system, and culture embryos safely for up to 7 days at 2-min intervals.

3 | MAIN FINDINGS

3.1 | Morphokinetic features in human embryos

3.1.1 | Process of fertilization and early embryonic development (Movie S1)

The detailed fertilization process and subsequent early embryonic development were revealed by the analysis of the hR-TLC images after cIVF. The following features can be observed in Movie S1, which is one of the best examples of the images obtained from the embryo for therapeutic purpose.[2,3]

The fertilization process in cIVF

We have previously demonstrated that most of the spermatozoa that penetrate the ZP immediately attach to the oolemma; after that, it takes approximately 40 min from the sperm-oolemma attachment to the disappearance of the sperm head (sperm-egg fusion). After the sperm head fuses into the oocyte membrane, the sperm tail still appears to be present in the perivitelline space (PVS) for approximately 20 min and thereafter disappears almost at the same time with the extrusion of the 2nd polar body (PB). The extrusion of the 2nd PB is completed within approximately 30 min. The fusion of the equatorial segment of the sperm into the oocyte membrane has also been described by R. Yanagimachi in the late 1980s.[12]

Fertilization cone

Experiments in rodent oocytes have revealed that a conical projection, the so-called fertilization cone (FC), appears at the sperm entry point (SEP).[13,14] The FC appears before the disaggregation of sperm chromatin and disappears after the completion of the chromatin disaggregation.[15–17] In 2006, by employing hR-TLC observation, we described for the first time in the literature that this phenomenon of the FC protrusion at the SEP also happens in human cIVF oocytes.[2,3,5] The FC in human oocytes appears almost 30 min after the commencement of the 2nd PB extrusion and continues existing

for 2 h, followed by the appearance of a cytoplasmic flare (described in the next section).[2,3] FC has been suggested to be a phenomenon that occurs through the interaction between the oolemma and the sperm. However, the detailed mechanisms and physiological function of the FC remain unknown.

Cytoplasmic flare

When the disaggregation of sperm chromatin starts after sperm penetration, a centrosome assembles the sperm aster by microtubule polymerization and induces migration of the pronuclei (PN; pronucleus or pronuclei, both abbreviated by PN).[18–21] Based on the continuous observation of human embryos at the early development stage using TLC, Payne et al. described a glassy cytoplasmic appearance radiating out from the center of the oocyte after ICSI as a cytoplasmic flare (flare).[1] In our hR-TLC analysis, flares were confirmed as the radiation and diffusion of cytoplasmic granules from the SEP immediately after the disappearance of the FC.[2–4] It is known that PN migration and abutment in the oocyte occur along the microtubules extended from the centrosome originating from the sperm (sperm aster) in some mammals, including humans.[19] In our hR-TLC analysis, the appearance of both male PN (mPN) and female PN (fPN) simultaneously with or shortly after the appearance of the flare from the SEP and the prompt migration of fPN toward mPN were observed. It is thought that the flare visually manifests the dynamics of the sperm aster.[2–4]

Translucent zone in peripheral ooplasm (halo)

After the fusion of the mPN and fPN, granular material in the ooplasm rapidly migrates to the surrounding area of both PN, resulting in the appearance of a translucent area (halo), which is markedly reduced granular material around the peripheral area of the ooplasm. The halo is considered to be a morphological change that indicates the migration of the mitochondria and other cell organelles along microtubules into the surrounding area of the PN.[1] Mitochondria in early human embryos assemble around the PN from the fusion of both PN to the syngamy and diffuse throughout the ooplasm after the syngamy.[21] It has been reported that mitochondria are abundant at the tip of daughter cells during the 1st cleavage and assemble around the nucleus in all blastomeres, once the cytoskeleton is complete.[22] Therefore, the halo captured by hR-TLC may be a manifestation of mitochondrial dynamics, and the relationship between the appearance of the halo and embryo quality as well as clinical outcomes is still controversial.[23,24] Nonetheless, it has been suggested that either the absence of halo or its appearance for a longer time had a negative correlation with the live birth rate after fresh cleaved embryo transfer. Overall, the characteristics of the cytoplasmic halo can be utilized to select more competent embryos for transfer at the cleavage stage.[24]

Nucleolar precursor body

Nucleolar precursor bodies (NPBs) appearing in the PN can be clearly observed under the microscope, and dynamic analysis by hR-TLC confirmed for the first time that NPBs move intensely in and out of the PN. Nucleoli in the nucleus of eukaryotes are involved in ribosomal ribonucleic acid (rRNA) transcription and ribosome biogenesis,[25,26] but the role of NPBs in embryonic development remains unclear. However, recent studies have shown that NPBs play an important role in pronucleation, a function quite different from that of nucleoli.[27,28] It has been suggested that the behavior of NPBs may be an indicator of embryo quality assessment, but this concept is still under debate.[29,30]

The pronuclear axis and the first cleavage plane formation (Movie S2)

According to the analysis of the embryos from the pronuclear stage to the 1st cleavage by hR-TLC, we found that the formation of the 1st cleavage plane can be defined by the 2PN axis, that is, a straight line between the centers of the mPN and the fPN. In our study,[31] it was shown that the majority of 2PN embryos (84.4%, 427/506) formed a cleavage plane parallel to the 2PN axis at the 1st cleavage and that these embryos had a high probability of developing into good-quality embryos and a significantly higher pregnancy rate after embryo transfer ($p < 0.01$). On the other hand, although a few embryos (5.9%, 30/509) were classified in the intermediate pattern, 9.7% of embryos (49/506) had the cleavage plane occur at perpendicular angles to the 2PN axis, and these were morphologically poor quality embryos followed by only 3 pregnancies (Figure 2 and Table 1).

In addition, in our fluorescent immunostaining of 2PN zygotes just before syngamy (Figure 3), most of the zygotes (11 out of 12 zygotes; Pattern A) showed two centrosome signals near the interface of the 2PN. These were thought to be the duplicated centrioles, which are the core structure of the centrosomes. The remaining zygote with the differentiated pattern (Pattern B) showed two pericentrin signals; one was located around the interface between the mPN and fPN, while the other was located distinctly distant from the junction of the 2PN (Figure 3). A spindle pole would form away from the pronuclear junction of pronuclei in this zygote, suggesting that the 1st cleavage plane is not parallel but perpendicular to the alignment of the mPN and fPN.[31]

Since each centriole is involved in a spindle pole that regulates chromosome segregation and cytoplasmic division,[32,33] the formation of the first cleavage plane parallel to the 2PN axis may be a predictive indicator of normal embryonic development.

3.1.2 | Observation of embryonic development from cleavage stage to hatched blastocyst

Several new findings that play an important role in the development of early human embryos were revealed by analysis of this period using hR-TLC and are presented below in detail.

The timing of compaction initiation

Compaction is thought to be the first apparent event in the differentiation of mammalian embryos and, in turn, has an important

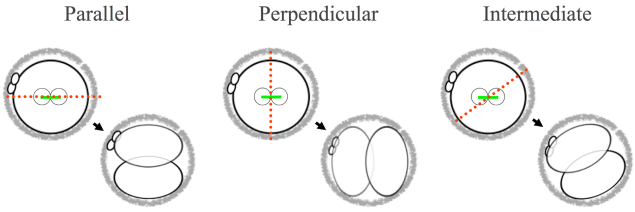

Embryos showed suitable imaging (n=506)		
Parallel	Perpendicular	Intermediate
84.4 % (427/506)	9.7 % (49/506)	5.9 % (30/506)

FIGURE 2 Different pattern of cleavage furrow on the 1st cleavage to the pronuclear axis. The light green color line indicates the two PN connection which is defined as the 2PN axis. The red dashed line indicates the angle of the 1st cleavage plane. Based on the direction of the first cleavage relative to the 2PN axis, 506 embryos that showed suitable images were further classified into three groups such as "parallel," "perpendicular," and "intermediate" (as shown in the table in the bottom panel). Our analysis revealed that most zygotes formed a cleavage furrow parallel to the 2PN axis (84.4%), suggesting that the two replicated centrosomes are often present near the pronuclear junction at the time of pronuclear breakdown (syngamy), resulting in the formation of the 1st cleavage plane formation parallel to the alignment of the mPN and fPN. Changes in centrosome positioning can lead to a cleavage furrow formation that is not parallel to the 2PN axis in some embryos, such as perpendicular pattern (9.7%) or intermediate (5.9%). fPN, female pronucleus; mPN, male pronucleus; PN, pronuclei.

TABLE 1 The comparison of pregnancy rate between parallel and perpendicular group.

Pregnancy rate	Parallel ($n=470$)	Perpendicular ($n=34$)	p value[a]
Fresh-ET	24.2% (45/186)	0% (0/14)	<0.05
Thawed ET	39.4% (112/286)	15.0% (3/20)	<0.05
Total	33.4% (157/470)	8.8% (3/34)	<0.01

[a]Chi-square test; $p<0.05$ confers statistical significance.

influence on the subsequent processes of blastocyst formation, the initiation of inner cell mass (ICM) formation, and trophectoderm differentiation.[34–42] Although compaction has been studied in several experimental animals (mouse, rabbit, bovine, rhesus monkey, etc.),[34–42] the timing and details of the onset of compaction during human embryonic development have not been elucidated. Our hR-TLC analysis provided new insights into the timing and behavior of compaction initiation in human embryos.[43] In principle, compaction in human embryos began after the third cleavage in the majority of embryos examined (99/115; 86.1%), most frequently at the 8-cell stage (26/115; 22.6%), and was widely distributed from the 8-cell to 16-cell stage (99/115; 86.1%). However, during the analysis, a small number (16/115; 13.9%) of embryos started compaction before the 8-cell stage or less, and the subsequent embryonic development of these embryos was extremely poor. The etiology of poor embryonic development is related to the formation of multinucleated blastomeres (MNB). Details of this finding have been described by K. Iwata et al.[43]

Development up to the blastocyst stage and the process of hatching (Movie S3)

A 2-cell stage embryo donated for research purposes was used to study blastocyst formation and the process of hatching. After thawing, the embryo was cultured and observed by hR-TLC for 5 days. During the observation of the embryonic development of this 2-cell stage embryo, it was observed that after compaction, the embryo developed into morula, followed by the formation of the blastocoel cavity, which is the blastocyst stage. The diameter of the blastocoel cavity gradually increased, and the embryos reached the full blastocyst stage with sporadic collapse of the cavity, and finally developed into an expanded blastocyst. ICM was clearly observed on the trophectoderm membrane during the blastocyst stage. As the blastocoel cavity expanded, the surrounding ZP became thinner and thinner, and a crack appeared in the ZP due to the slight collapse of the blastocoel cavity and the blastocyst escaped through the site of a crack in the ZP (hatching). The hatching process took approximately 7 h and 25 min. This series of images of the development process up to the hatching of the blastocyst was described and confirmed for the first time by hR-TLC observation.[3]

3.1.3 | Time course of embryonic development from insemination to 2nd cleavage in in vitro culture conditions (Figure 4)

The time course of human oocyte development from insemination to the 2nd cleavage by fertilization under in vitro culture conditions was determined from the analysis of hR-TLC images.[2,3]

We analyzed the serial time course from insemination up to the 2nd cleavage. As previously described,[2,3,5] the hR-TLC monitoring was commenced at 1.5 h post-insemination (images taken at 10-s intervals until the sperm were incorporated into the ooplasm) and continued at 2-min intervals for approximately 40 h. Surprisingly, human sperm can pass through the ZP faster than we expected, as the required time was approximately 1.5 h post-insemination. The extrusion of the 2nd PB occurred at 2.5 h post-insemination, which was determined as oocyte activation by the presence of substances from the sperm [sperm factor; currently known to be phospholipase C-zeta (PLC-z)].[44] Human zygotes reached syngamy at 24.4 h post-insemination and the 1st cleavage at 26.8 h post-insemination after a series of physiological events. The 2nd cleavage, 2nd mitotic division, occurred 10 h later.[2,3]

Although the time course from the 2nd PB extrusion was not significantly different between cIVF and ICSI, the time required for sperm entry into the oocytes for the 2nd PB extrusion was delayed by 1 h in

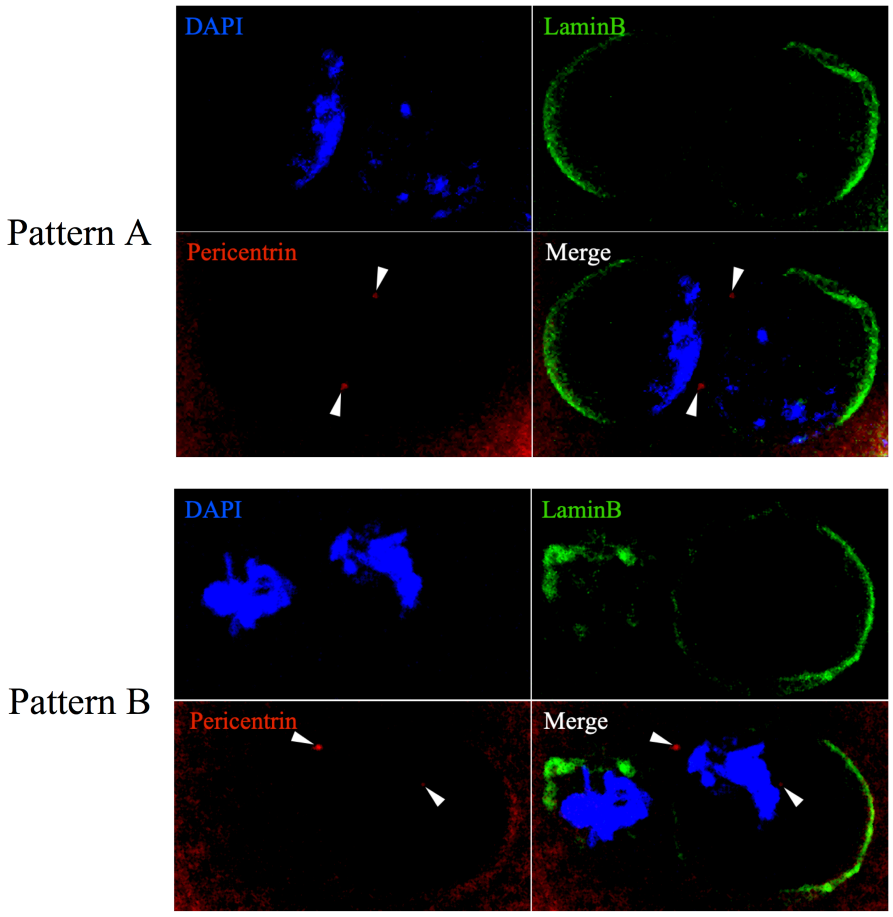

FIGURE 3 Localization of the centrosome during the pronuclear phase of normally fertilized human oocytes. Pattern A: Immunofluorescence staining for DAPI, lamin B, and pericentrin in a normally fertilized human oocyte. The upper left panel shows the nuclear DNA stained with DAPI (blue, Hoechst). The upper right panel shows lamin B localization at the PN periphery stained green. In the lower left panel, two pericentrin-positive centrosomes are present, which emit signals in red color and are marked with white arrowheads. The centrosomes appear to be aligned around the interface between the mPN and the fPN. Pattern B: Immunofluorescence staining for DAPI, lamin B, and pericentrin in normally fertilized human oocyte. The upper left panel shows the nuclear DNA stained with DAPI (blue, Hoechst). The upper right panel shows lamin B localization at the PN periphery stained green. In the lower left panel, two pericentrin-positive centrosomes are present, which emit signals in red color and are marked with white arrowheads. It appears that one of two detected pericentrin signals was detected around the interface between the mPN and the fPN, and the other was clearly distant from the interface of the two PN. DAPI, 4′-6-Diamidino-2-phenylindole; fPN, female pronucleus; mPN: male pronucleus; PN, pronuclei.

ICSI, probably due to the super-physiological and invasive nature of sperm injection in the ICSI procedure. Therefore, this suggests that the ICSI procedure may affect the early stage of oocyte activation.

3.1.4 | Two types of hatching patterns in the blastocyst stage (inward and outward) (Movie S4)

The escape of expanded blastocysts from the ZP (hatching) is an epilogue of embryonic development prior to implantation. Although several hypotheses have been proposed regarding the mechanism of hatching in mouse, bovine, equine, and human,[45–47] the actual process remains unknown. Two novel hatching patterns, termed "inward" and "outward," were revealed by the hR-TLC observation, using donated day-2 frozen/thawed embryos, which were cultured up to the hatching stage.

In the "inward" pattern, after a fully expanded blastocyst has developed, the blastocoel cavity suddenly collapses, and simultaneously, the ZP retracts inward, followed by a break in the ZP. The blastocyst escapes through the rupture site as the blastocoel cavity continues to expand.

In the clinical setting, artificial collapse of the blastocoel cavity is widely applied in blastocyst cryopreservation. However, spontaneous blastocoel collapse is generally considered to have a negative effect on embryonic development by the observation of hR-TLC.[4,48] It has been confirmed that blastocysts with repeated major collapses have a high probability of poor subsequent development, failure to reach hatching and a lower live birth rate. Nevertheless, the blastocyst multiple collapse pattern is not recommended to be evaluated alone as a predictor of the reproductive outcome, but the morphokinetic variables should also be taken into account.[49]

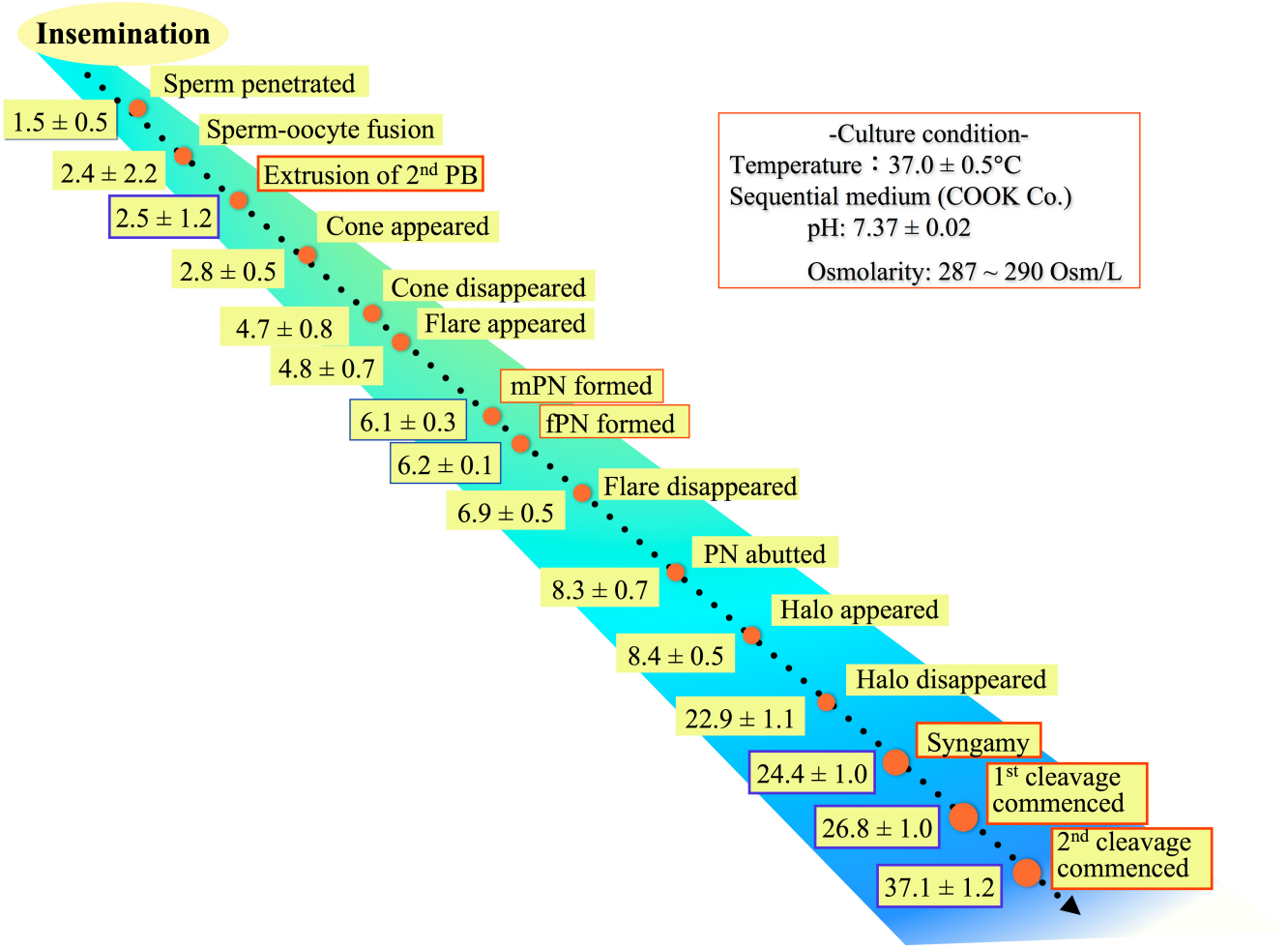

FIGURE 4 Time course of embryonic development from insemination to 2nd cleavage in an in vitro culture condition after cIVF. On the left side of the dotted line the numbers in the boxes indicate post-insemination h ± SD. cIVF, conventional in vitro fertilization; cone, fertilization cone; flare, cytoplasmic flare; fPN, female pronucleus; halo, translucent zone in the periphery of the ooplasm; mPN, male pronucleus; PB, polar body; PN, pronuclei; SD, standard deviation.

On the other hand, in the "outward" pattern, the blastocoel cavity first expands gradually without any collapse of the blastocoel cavity, then the ZP is ruptured and the blastocyst escapes rapidly through the rupture site.[5] When we first described the hatching patterns, we noticed that the "inward" pattern was more prevalent than the "outward" pattern, while the latter required less time to hatch. Although most of the blastocysts that escaped from the ZP showed an inward pattern under in vitro culture conditions, it is still interesting to know what the hatching style is in in vivo culture.

3.2 | Atypical morphokinetic features involved in further embryonic development observed by hR-TLC

3.2.1 | Period from fertilization to 2PN formation

Several atypical phenomena that may affect subsequent embryonic development during the period from fertilization to pronuclear formation are discussed in detail in the following sections.

Single pronuclear zygote (1PN zygote) by the excessive extrusion of female pronuclear materials (Movie S5)

Zygotes with a single PN (1PN zygote) are one of the most frequent and atypical features involved in further embryonic development. Previously, it has been reported that 1PN zygotes occurred in (1) parthenogenesis,[50,51] (2) asynchronous or delayed formation of pronuclei,[52] and (3) diploid chromosome complement within 1PN.[52,53] In addition, it has also been reported that healthy babies were born after the embryo transfer (ET) using 1PN zygotes.[54–56] However, in our hR-TLC analysis, a novel insight into the etiology of the 1PN zygote was obtained, namely, the presence of an excessive extrusion of fPN materials (a third meiotic division-like phenomenon).

This feature was first observed in an oocyte after ICSI. In the hR-TLC image of this oocyte, the 2nd PB was extruded near the 1st PB approximately 2.5 h after ICSI, and, surprisingly, a PB-like material was also extruded next to the 2nd PB. Simultaneously, a single PN was formed in the ooplasm, which seemed to be the mPN. A PB-like material remained in the PVS next to the 2nd PB

during the zygote stage. It was strongly suggested that the PB-like material contained fPN substances and was extruded as a 3rd PB, although the chromosomal status of the 3rd PB-like material was not confirmed by immunostaining methods. This phenomenon indicates that a 3rd mitotic division exists, that is, the excessive extrusion of a 3rd PB, and occurs in human embryos. If that were possible in real feature, the zygote would contain half of the chromosomes and should not be used clinically. In fact, that specific zygote had severe fragmentation after the first cleavage and stopped developing thereafter.

Uneven 2PN zygote (Movie S6)

In the clinical setting, after fertilization is confirmed on day 1 [the next day after the day of OPU (day-0)], zygotes with two unequal-sized PN are sometimes encountered. The etiology and normality of these zygotes are highly controversial.[57] However, we have obtained extremely rare and valuable images of the mechanism of this feature through our hR-TLC analysis.

As the extrusion of the 3rd PB described above, this was also an extraordinary feature, and we were extremely surprised when we observed it. In this zygote obtained by ICSI, the 3rd PB-like material was extruded next to the 2nd PB. In addition, at the same time that the PN, which would be the mPN, was formed in the center of the ooplasm, a small PN-like substance containing NPB-like materials was also formed in the 3rd PB. Subsequently, this PN-like substance was reabsorbed into the ooplasm and moved toward the PN (mPN) in the ooplasm. Finally, both abutted and formed an uneven 2PN within the ooplasm.[4] It appeared that a small, PN-like substance was clearly extruded into the PVS. However, without evidence of a mechanism for the connection between the ooplasm and the PN-like substance, it was thought that this event did not occur. Therefore, it is possible that the PN-like substance was not completely interrupted and was able to communicate with the ooplasm. Further research on this topic has not yet been conducted, but it would be of great importance to shed light on this feature.

Zygotes with three or more PN

On day-1, the most frequently encountered abnormal fertilization was zygotes with three or more PN. Our hR-TLC analysis showed that there were three etiologies: (1) polyspermy, (2) failure of 2nd PB extrusion, and (3) fragmentation of PN.

Polyspermy. Polyspermy is fertilization by more than one sperm and is one of the most common irregular features during the fertilization process in in vitro fertilization. The oocytes, in which polyspermy was confirmed, were identified as having three or more PN at a fixed time point during the fertilization status assessment on day 1. According to hR-TLC image analyses,[1,58] the diameter of the mPN was slightly larger than that of the fPN (28.1 ± 2.0 μm, 26.4 ± 2.0 μm, respectively). These data suggest that it is possible to identify the number of sperm that fertilized the oocyte by measuring the PN diameters. If the oocyte contained two or more larger PN and one smaller PN, the condition was evaluated as polyspermy. If the oocyte contained one larger PN and two smaller PN, the oocyte probably failed to extrude the 2nd PB after a single sperm entered the ooplasm, meaning that a "failure of 2nd PB extrusion" occurred, as described below.

In 2017, we had the opportunity to use a 4K camera (courtesy of Japan Broadcasting Corporation; NHK) attached to the in vitro culture system for hR-TLC. While observing the fertilization process using oocytes after insemination by hR-TLC with a 4K camera, we found a clear and remarkable image in which two different spermatozoa simultaneously entered the oocyte (time difference between two spermatozoa: 30 s) (Movie S7).

In 2012, analysis of the fertilization process using hR-TLC provided new insights into the possible mechanism of the polyspermy block.[59] In mammalian fertilization, it is thought that the main mechanism for preventing polyspermy is the zona reaction, which is the hardening of the ZP by the absorption of cortical granules. Cortical granules are extruded into the PVS by infusion of PLC-z from the sperm attached to the oocyte membrane.[44,60,61] However, the analysis of hR-TLC images showed that the ZP penetration by the following sperm was inhibited within 10 s after the leading sperm attached to the oocyte membrane. This suggests the existence of a possible mechanism for the polyspermy block, which has been completely unknown until that moment. Further research is needed to elucidate this mysterious phenomenon.

Failure of 2nd PB extrusion. In clinical practice, novel phenomena strongly suggest that the occurrence of zygotes with 3PN may be due to a failure of the 2nd PB extrusion. Unfortunately, although these features could not be captured by our hR-TLC, they were confirmed at the fertilization check on day 1 by using an incubator equipped with time-lapse monitoring (time-lapse incubator). At that time, we detected two possible mechanisms involved in the failure of the 2nd PB extrusion: (1) reabsorption of the 2nd PB after extrusion, and (2) the failure of the 2nd PB extrusion itself (Figure 5). In the fertilization process, the oocytes are activated by sperm incorporation and resume the second meiotic division, which is completed by the 2nd PB extrusion.[62] However, it is thought that the second meiotic division does not work properly and exhibits unusual dynamics in some oocytes. The extrusion of the 3rd PB related to 1PN zygotes or the failure of the 2nd PB extrusion involved in 3PN zygotes may be an extremely unusual and rare phenomenon in reality, but they give us a glimpse of the complexity and mystery of the fertilization process and the mechanism of early embryonic development.

Fragmentation of PN. A very interesting phenomenon that we could also observe with our hR-TLC system was the formation of zygotes with multiple PN (three or more). This phenomenon was probably a result of (1) fragments of the PN itself, and (2) failure of the 2nd PB extrusion combined with fragmentation of the PN at the time of fertilization confirmation after ICSI on

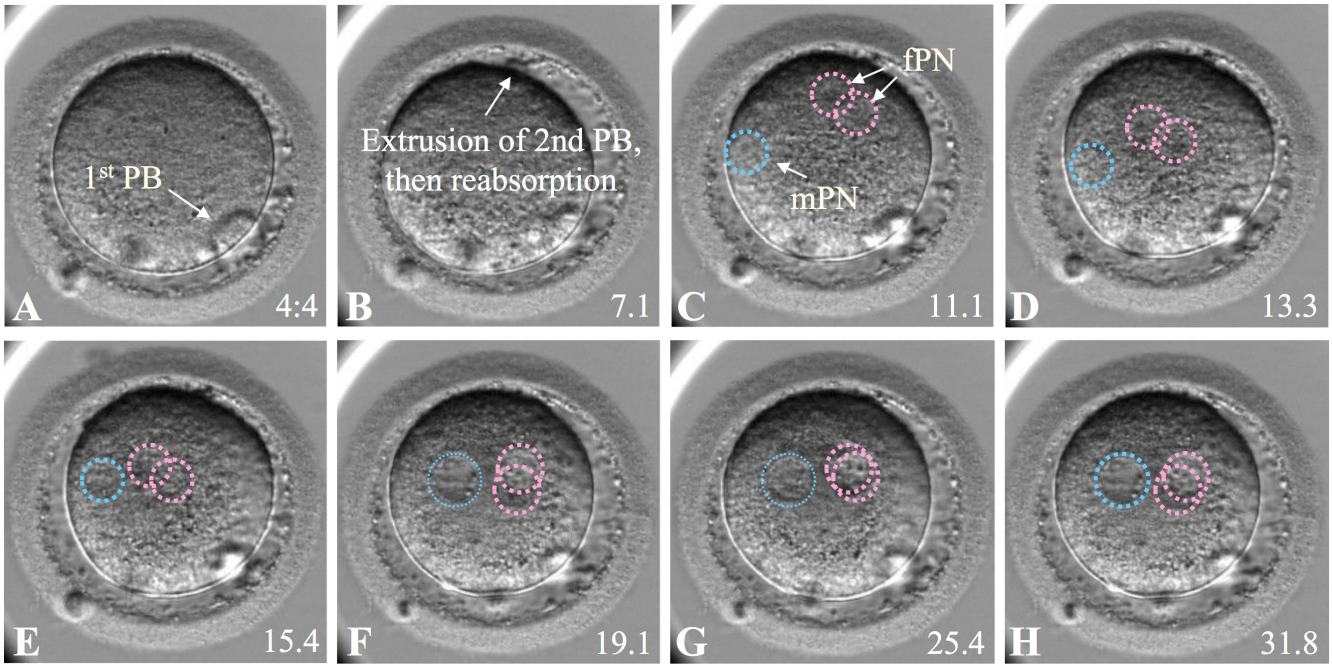

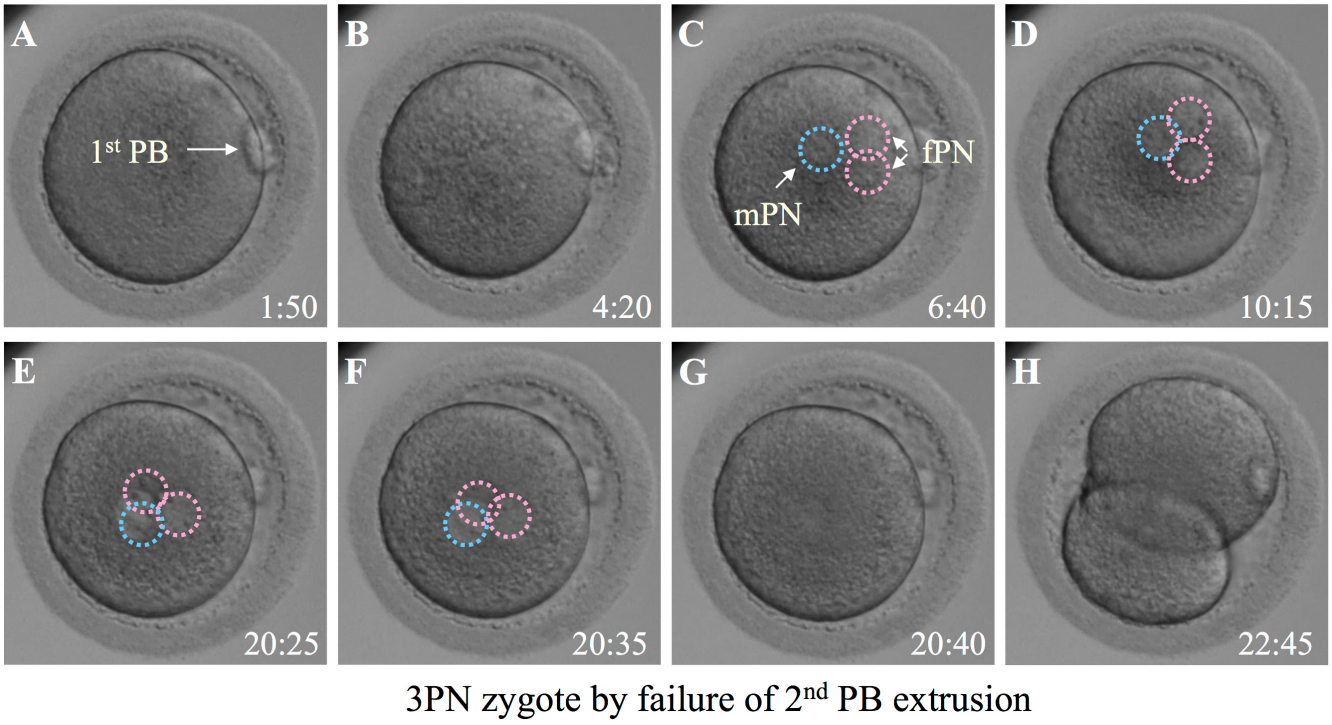

FIGURE 5 3PN zygote due to failure of 2nd PB extrusion. 3PN zygote due to reabsorption of 2nd PB after 2nd PB extrusion. (A) The 1st PB was located in the PVS as indicated by the arrow. (B) The 2nd PB was extruded at the 1 o'clock position. However, the 2nd PB was resorbed 2.7 h later. (C) A single mPN (marked with light blue dashed circle) and two fPN (marked with pink dashed circle) appeared 4 h after reabsorption of the 2nd PB (3PN zygote). (D–H) The state of 3PN state persisted for more than 20 h. 3PN zygote due to failure of 2nd PB extrusion. (A,B) The 1st PB was seen at the 3 o'clock position in the PVS as indicated by the arrow. (C–F) A single mPN and two fPN appeared approximately 5 h later. There was no extrusion of the 2nd PB. (G) The three PN disappeared (syngamy) 14 h after the appearance of 3PN. (H) The 1st cleavage occurred 2 h after syngamy. fPN, female pronucleus; mPN, male pronucleus; PB, polar body; PN, pronucleus; PVS, perivitelline space.

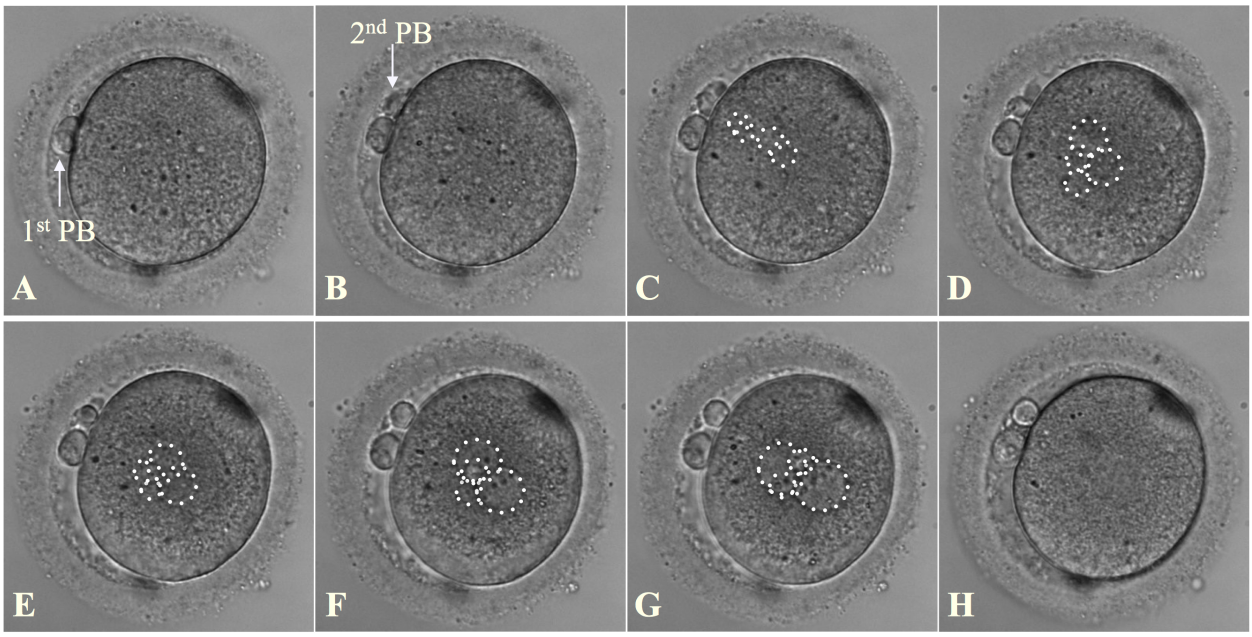

FIGURE 6 Two types of poly-pronuclear zygotes with PN fragmentation. Poly-pronuclear zygotes with fragmentation of the PN. (A,B) The 2nd PB was extruded next to the 1st PB (Panel A: the 1st PB is marked with a white arrow; Panel B: the 2nd PB is marked with a white arrow and it is located next to the 1st PB in the PVS). (C,D) Four small diameter PN (indicated by white color dashed circles) appeared and then abutted. (E-G) Each PN (indicated by white color dashed circles) gradually increased in size. (H) All PN disappeared simultaneously. Poly-pronuclear zygotes with failure of the 2nd PB and fragmentation of the PN. (A,B) The 2nd PB was not extruded and the cytoplasmic flare, indicated by 3 black arrows, appeared at the 5 o'clock position (in panel A the 1st PB is indicated by a black arrow). (C) Three PN of different sizes (indicated by white color dashed circles) appeared in the ooplasm. (D–F) Subsequently, the number of PN (indicated by white color dashed circles) increased up to a maximum of 8 and then all disappeared simultaneously. PB, polar body; PN, pronucleus/pronuclei; PVS, perivitelline space.

day-1 (Figure 6). Since these zygotes were formed from oocytes injected each with a single spermatozoon by ICSI and had already released their 2nd PB, and since the size of the PN was uneven in size, the fragmentation of the PN was the most likely explanation. However, there is still no clear explanation for this phenomenon and further research is necessary.

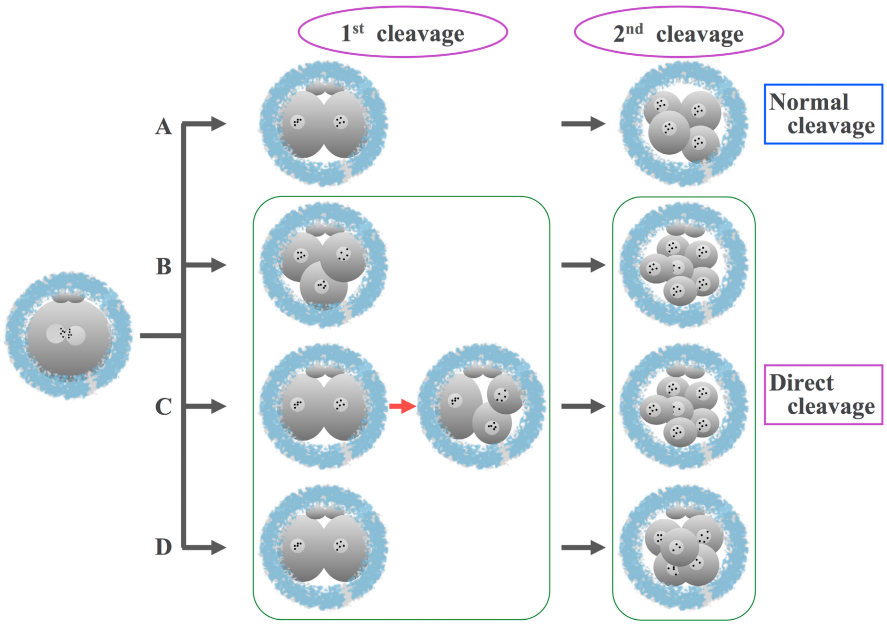

FIGURE 7 Three types of direct cleavage pattern during the 1st and the 2nd cleavage. In the analysis of the direct cleavage, it was confirmed that there were 3 types of cleavage pattern in direct cleavage.

TABLE 2 Clinical outcomes in normal and direct cleavage.

	Rate of occurrence (%)	Age (mean ± S.D.)	Clinical pregnancy (%)	Live birth (%)	Miscarriage (%)
Group 1 (Normal cleavage, 1 → 2) ($n = 739$)	83.6 (739/884)	37.4 ± 4.9	36.3 (268/739)	28.4 (210/739)	21.6 (58/268)
Group 2 (Direct cleavage, 1 → 3) ($n = 34$)	3.8 (34/884)	39.1 ± 5.2*	0** (0/34)	–	–
Group 3 (Direct cleavage, 1 → 2 → 3) ($n = 52$)	5.9 (52/884)	38.6 ± 6.0	25.0 (13/52)	13.5** (7/52)	46.2** (6/13)
Group 4 (Direct cleavage, 2 → 5) ($n = 59$)	6.7 (59/884)	38.7 ± 5.1*	18.6** (11/59)	15.3** (9/59)	18.2 (2/11)

Note: * and ** $p < 0.05$ and $p < 0.01$ confer a statistically significant difference, respectively, compared to Group 1 (Chi-square test). Group 2 resulted in no pregnancy, but Groups 3 and 4 resulted in some successful pregnancies and live births. Therefore, it is important that 2-cell stage should occur at the early cleavage stage.

3.2.2 | Period from PN formation to early cleavage

During this period, the most common unusual features are (1) direct cleavage, and (2) fragmentation.

Direct cleavage (Movie S8)

Normally, human zygotes initiate the first cleavage approximately 2 h after syngamy and repeat cell divisions approximately every 10 h thereafter. In 2012, Rubio et al. reported that the implantation rate of zygotes that develop from 2-cell to 3-cell or more within 5 h after the 1st cleavage (direct cleavage; DC) was significantly lower than that of zygotes with a normal cleavage pattern (20.2% vs. 1.2%, $p < 0.0001$).[63] Based on our analysis using hR-TLC as well, zygotes with direct divisions at the first (1-cell to 3-cell or more; DC1-3) and second (2-cell to 5-cell or more; DC2-5) cleavages (with confirmed nuclear formation in every blastomere) were observed (Figure 7), and zygotes with direct divisions at the 1st cleavage did not result in pregnancy. Thus, morphokinetic analysis enables the identification of irregular divisions in the early cleavage embryos.

However, it was reported that some direct-cleaved zygotes at the 1st cleavage could still lead to a live birth.[64] Therefore, we conducted a more detailed analysis on early cleavages and confirmed two types of irregular 1st cleavages: (1) a cleavage from 1-cell to 2-cell, and then from 2-cell to 3-cell or more within 5 h after the 1st cleavage (DC1-2-3), and (2) a direct cleavage from 1-cell to 3-cell or more (DC1-3). DC1-3 zygotes did not result in pregnancy, while DC1-2-3 zygotes resulted in some cases with successful pregnancy and live birth. Therefore, some of the DC1-2-3 zygotes possibly have at least one blastomere with a normal number of chromosomes at the 2-cell stage, and that viable zygotes result in live birth (Table 2). Similar irregularities during the 2nd cleavage may occur in DC2-5 zygotes, resulting in pregnancy and live births. Nevertheless, it is necessary to be prudent when clinically utilizing zygotes with DC.

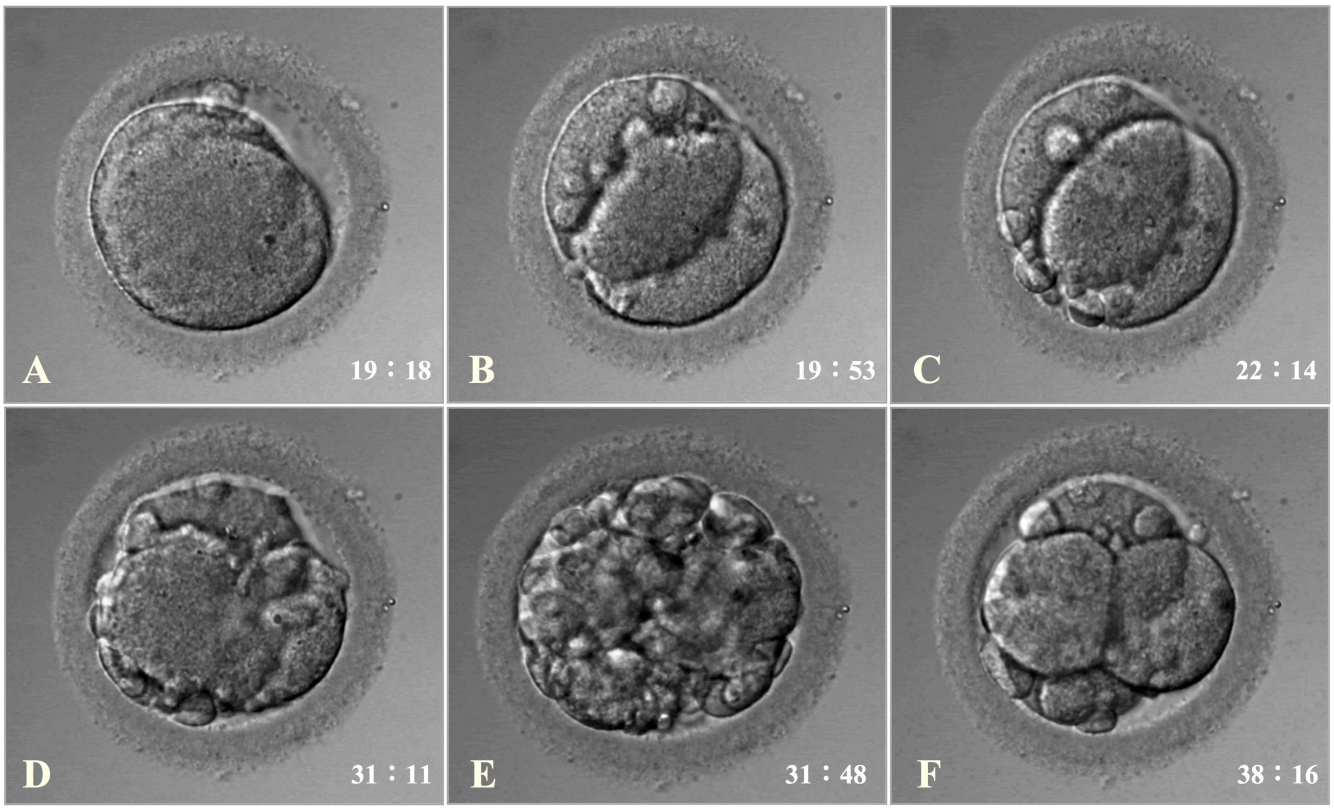

FIGURE 8 Fragmentation generated along the cleavage furrow. 1st cleavage. (A) The cleavage furrow appears at 19 h and 19 min. (B,C) During the 1st cleavage, fragments are generated along the cleavage furrow, but after 2 h and 22 min, fragmentation was evidently reduced. 2nd cleavage. (D) The 2nd cleavage starts at 31 h and 11 min after the beginning of the observation. (E,F) During the 2nd cleavage, fragmentation intensively occurs, but the fragments are apparently reduced and the embryo recovers to good quality after 6 h and 28 min.

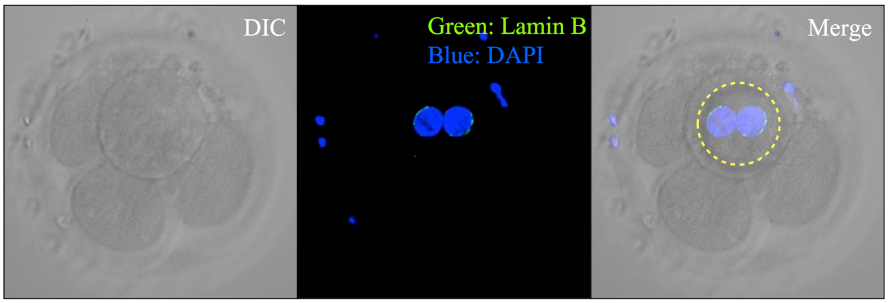

Cytokinetic failure with karyokinesis

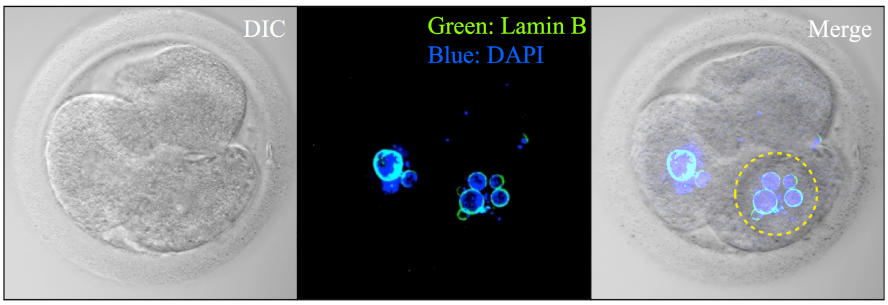

Fragmentation/failure of nuclear membrane in blastomeres

FIGURE 9 Immunostaining of nuclei and nuclear membranes in two types of multinucleated blastomeres. In the upper panel (cytokinetic failure with karyokinesis): two equal-sized nuclei were stained with anti-lamin B_1 (green color) and DAPI (blue color, Hoechst) in the blastomere (upper middle and upper right frames). In the lower panel (fragmentation/failure of nuclear membrane in the blastomeres): two blastomeres had multiple nuclei of different sizes as shown by staining with anti-lamin B_1 (green color) and DAPI (blue color, Hoechst) in the lower middle and lower right frames. DNA is counterstained with DAPI (blue) and the nuclear membrane is counterstained with lamin B_1 (green). DAPI, 4′,6-diamidino-2-phenylindole; DIC, differential interference contrast.

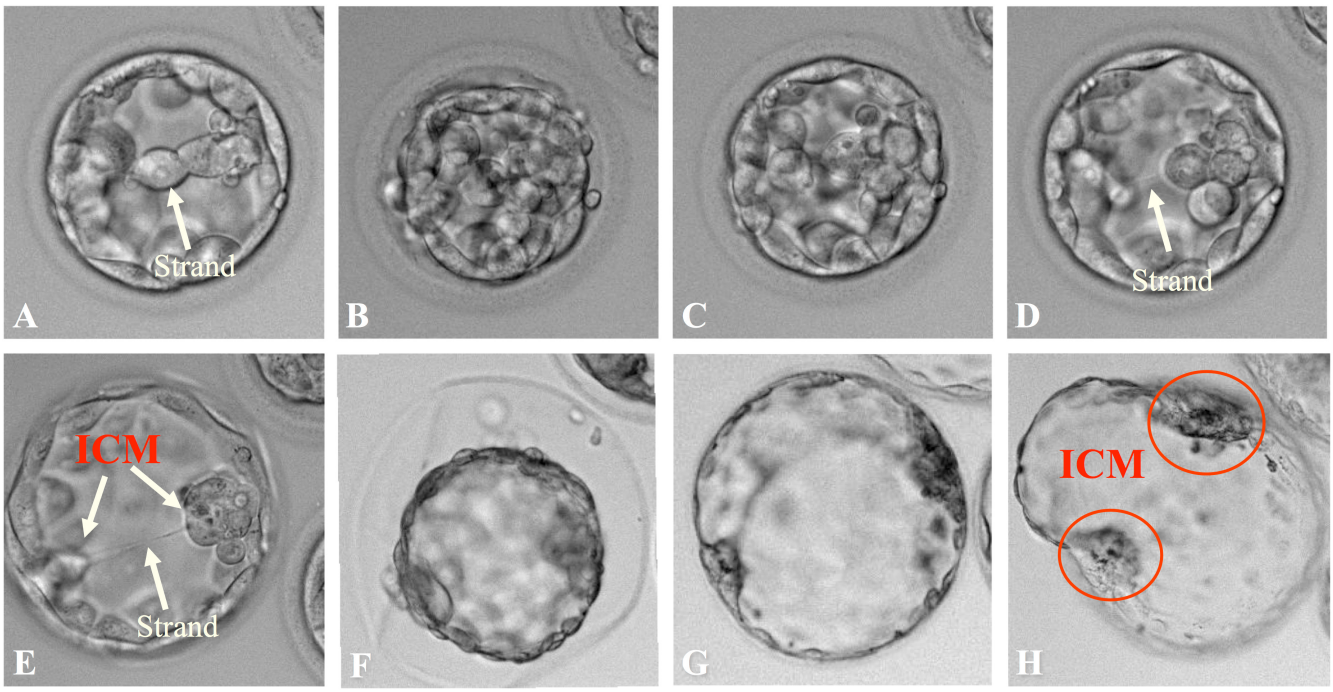

FIGURE 10 Splitting of the ICMs caused by the strand phenomenon during the blastocyst stage (monozygotic twinning). (A) During the formation of the blastocoel cavity, the ICM adhered to the opposite side of the trophectoderm, resulting in a "strand" indicated by the white arrow. (B–D) The blastocoel cavity collapsed, followed by repeated collapse and re-expansion (white arrow points to the strand). (E–G) The ICM was separated and 2 ICMs (indicated by red arrows) formed in the blastocoel cavity (in panel E white arrow indicates the strand). (H) The blastocyst with 2 ICMs (marked with red color circles) escaped through the zona pellucida. ICM, inner cell mass.

We should avoid freezing or transferring these zygotes on day 2 or−3; culture them for a longer period to confirm the blastocyst development, and carefully consider the priority order of the embryos for use.[63]

Fragmentation

Numerous studies have reported that increased amounts of fragments at the early cleavage stage adversely affect further embryonic development and subsequent clinical outcomes.[65,66] However, the mechanism involved in fragmentation has not been fully elucidated. Dynamic analysis of human embryos has now revealed two possible mechanisms of fragmentation.

Fragmentation generated along cleavage furrow. Our detailed analysis revealed that fragments were generated along the cleavage furrow during the 1st and 2nd cleavage, and the number of fragments sometimes decreased with time due to the resorption of fragments into the blastomere.[4] In addition, based on our chronological analysis of the number of fragments after cleavage, we confirmed that the massive number of fragments generated during cleavage significantly decreased at approximately 2 h, and the resulting embryo was of good quality (Figure 8). Therefore, it is important to re-evaluate poor-quality embryos with a massive number of fragments at intervals of approximately 2 h.[4,67]

Fragments generated at the perivitelline threads (PT). In 2017, thin filaments defined as PT extending across the PVS and connecting the ZP to the ooplasmic membrane were reported to be one of the causes of fragmentation based on an analysis of human embryos using a time-lapse incubator.[68,69] PT may play an important role in cross-linking the cumulus cells and the oocyte during maturation,[70] but the mechanism underlying such a role remains unclear.

Derrick R et al. used time-lapse imaging to observe PT in more than 50% of human embryos at the cleavage stage, and the rate of cytoplasmic fragmentation (at the 1st cleavage) was significantly reduced in embryos without PT.[68] Additionally, based on time-lapse observations of ICSI embryos obtained from ART treatments performed at our clinic, we confirmed the involvement of PT in the formation of cytoplasmic fragments during the 1st cleavage (Movie S9).[71] In contrast, Kellam L et al. found no significant difference in the rate of fragmentation between embryos with PT and those without PT at the two-cell stage.[69]

Nevertheless, detailed analyses using time-lapse imaging have shown that PT is clearly involved in the formation of cytoplasmic fragments during the first cleavage.[68,71] However, in the clinical setting, certain patients have only poor-quality embryos (PQE) due to severe fragmentation and cannot obtain any embryos used for embryo transfer and/or cryopreservation. To help these patients, we conducted a preliminary study to investigate the effectiveness of artificial removal of ZP (ZP-free) at the zygote stage using abnormally fertilized zygotes (3PN) that could not be used clinically. The results of the preliminary study showed that ZP-free embryos significantly reduced fragmentation in embryos from patients with PQE alone compared to the zygotes without artificial

removal of the ZP (ZP-intact) ($p < 0.01$).[71] The clinical efficacy of ZP-free treatment in patients with intractable infertility is currently being investigated.

3.2.3 | The third cleavage and beyond

During these stages of the embryonic development, several atypical features which were directly involved in further embryonic development were obtained from the analysis of hR-TLC observations.

Formation of MNB

The formation of MNB is frequently encountered as an irregular finding in early human embryos.[43] During the analysis of the early cleavage and compaction stages using hR-TLC, we identified a new phenomenon related to MNB development. As mentioned above, although in the majority of human embryos, compaction occurs after the 3rd cleavage, that is, after the 8-cell stage, in some embryos, compaction occurred at an earlier cell stage, albeit at a lower frequency, and these embryos showed poor further embryonic development. Detailed analysis of these embryos by hR-TLC revealed the existence of two patterns in the mechanism of MNB occurrence: (1) cytokinetic failure with karyokinesis, and (2) fragmentation of nuclear membranes in blastomeres.[43]

Cytokinetic failure with karyokinesis (early initiation of compaction). During the 3rd cleavage from the 4-cell stage in some of the blastomeres, a cleavage furrow occurred, and the blastomere was almost going to divide into two blastomeres. The division was interrupted, and the blastomere returned to its original form, a phenomenon called "cytokinetic failure." At that moment, two equal-sized nuclei appeared in the blastomere, indicating the formation of MNB. We speculated that the nucleus in the blastomere was duplicated and divided into two nuclei (karyokinesis), without cytokinesis. Therefore, the blastomere with MNB indicates that the nuclear phase has reached the 3rd cleavage, but the cytokinesis did not occur. Theoretically, if compaction began at the 7-cell stage, it means that this phenomenon occurred in only one blastomere; if it began at the 6-cell stage, this occurred in two 2 blastomeres; if it began at the 5-cell stage; it occurred in three blastomeres, and if compaction began at the 4-cell stage, all four blastomeres failed cytokinesis.[5,43]

Fragmentation/failure of nuclear membrane in blastomeres. Additionally, we identified embryos in which multiple unequal-sized nuclei containing nucleolus-like material appeared in each blastomere during early cleavage. We evaluated these embryos as clinically unusable, and with the patients' consent, they were used for research, and immunostaining was applied. Analysis using DAPI (4′,6-diamidino-2-phenylindole) for nuclear staining and Lamin B_1 for nuclear membrane staining indicated that each unequal sized nuclear-like material was a nucleus accompanied by a nuclear membrane (Figure 9).

Strand phenomenon (Movie S10)[3]

Our hR-TLC analysis after the blastocyst stage in human embryos confirmed for the first time an interesting phenomenon newly named the "strand phenomenon." In this phenomenon, the ICM and the opposite side of the trophectoderm adhere to each other and pull strings during blastocoel formation. Surprisingly, more than half of the blastocysts analyzed by hR-TLC showed this "strand phenomenon" to varying degrees in the blastocyst developed in vitro.[3] Although whether the same phenomenon occurs at the blastocyst stage in an in vivo situation is unknown, it may deviate from the physiological process or it may also occur in vivo as well. In addition, an in vitro culture condition in ART may not be as optimal for human embryos as the female uterus, although we are all working in that direction to make it as ideal as possible, and the extended in vitro culture up to the blastocyst stage may somehow cause stress to the embryos. Considering these issues, we cannot exclude the possibility that this phenomenon may be one of the adverse effects of extended in vitro culture.

New mechanism of monozygotic twin (MZT)

It has been reported that the ICM was separated by the hardened ZP during the hatching process.[72–74] However, for the first time, hR-TLC confirmed that a blastocyst with two ICMs[3] is formed during the blastocyst stage when a strand phenomenon occurs between the ICM and contralateral trophoblast, causing the inner cell mass to be separated (Figure 10).

In the clinical setting of ART, the frequency of MZT is significantly increased in blastocyst transfers compared to early embryo transfers.[73,74] This finding supports the conclusion that this is due to the strand phenomenon caused by an extended in vitro culture up to the blastocyst stage. In addition, if the occurrence of MZT is caused by the strand phenomenon during the blastocyst stage, this phenomenon is extremely risky, and an extended in vitro culture of human embryos would have a negative impact.

4 | CONCLUSIONS

The future is full of surprises and potential. Many researchers from different scientific fields from all around the world continue to put a lot of effort into developing new technologies in order to help assisted reproduction professionals provide the best medical care to their patients. HR-TLC, combined with the careful use of artificial intelligence (AI), can really help in enabling less invasive methods for selecting embryos that have a higher chance of implantation. To date, there are few studies showing the benefits of using AI in the observation and evaluation of human embryo preimplantation dynamics.[48,75–77] By establishing valid and effective algorithms for time-lapse incubators, we will be able to set stronger criteria that will qualify the prediction of normal growth and development potential of embryos, as well as the detection of aneuploidies, in order to avoid the application of invasive techniques such as preimplantation genetic testing.

At the dawn of a greener and more sustainable era in assisted reproduction and healthcare in general, we need to think and act wisely when it comes to the design and application of an AI-driven hR-TLC evaluation system. There is no doubt that AI can make some tasks in the embryology laboratory easier and faster. On the other hand, the enormous amount of data that is and will be collected will require more powerful computers for analysis, which means higher energy consumption, greater emissions of greenhouse gases, and ultimately harmful consequences for the environment and human health.

This review outlines 20 years of hR-TLC and all the events from human oocyte fertilization to blastocyst hatching, as well as atypical features that we had the opportunity to witness and report, some of them for the first time in the international literature. In 2003, about two years of trial and error, we developed a new in vitro culture system for hR-TLC that was able to maintain optimal and stable culture conditions on the microscope stage for periods of up to one week.[3,4] This analysis of early human embryos using hR-TLC allowed us to catch a glimpse of the miracle of life at its beginning and ushered in a new era for ART. Therefore, we have focused on the results of our original hR-TLC analysis and discussed them herein.

Several novel findings and phenomena described in this review were elucidated by the analysis of hR-TLC images. Most of these phenomena could not be identified using fixed-time observation during in vitro culture and/or data from animal experiments.

All of the oocytes and embryos observed and analyzed by hR-TLC were the seeds of human life entrusted to us by the couples who wished to have child of their own. Therefore, experimental methods that do not comply with ethical guidelines or that do not show the appropriate respect in the handling of human embryos, regardless of their purpose and results, are unacceptable. It is necessary to consider the limitations of the research that can be applied according to the bioethics of human life. In our preliminary study of hR-TLC, no adverse effects of hR-TLC on embryonic development were observed, although these effects were derived from abnormally fertilized human oocytes. After obtaining approval from the JISART (Japanese Institution for Standardizing Assisted Reproductive Technology) Ethics Committee, we began the observation of human oocytes and embryos for clinical use. In fact, compared with the beginning of this research 20 years ago, the concept of the sanctity of life and bioethical regulations have become stricter, making the development of novel and effective research for human embryos more difficult. Under these circumstances, TLC is expected to become an increasingly important method for studying human embryonic development and for developing new therapeutic methods. In this context, we have recently established a new promising therapeutic approach based on TLC analysis, the ZP-free procedure.[71] This novel method has the ability to improve embryo quality deterioration due to severe fragmentation. Based on the preliminary results of our study on 3PN embryos we have started applying the ZP-free method clinically on fully informed patients with recurrent ART failure due to excessive fragmentation and we have achieved good results that soon will be published. Therefore, we have devoted our work to establishing strong criteria for the selection of zygotes suitable for the application of this novel procedure.

All the images obtained by hR-TLC will not only help in future scientific analysis of the mysteries of the beginning of life but can also serve as a source of education and learning about the origin of life and the dignity and awe of the birth of life.

ACKNOWLEDGMENTS

We would like to express particular thanks to Dianna Payne and Sean P. Flaherty in Adelaide, Australia, for their invaluable support in developing an in vitro culture system for high-resolution time-lapse cinematography and for the research collaboration all these years. We would also like to especially thank all of the embryologists at Mio Fertility Clinic for their excellent laboratory work and for the collection of data over the years.

CONFLICT OF INTEREST STATEMENT

The authors declare no conflict of interest.

APPROVAL BY ETHICS COMMITTEE

All the studies described in this review article were approved by the ethical committee of JISART (Japanese Institution for Standardizing Assisted Reproductive Technology).

HUMAN RIGHT STATEMENTS AND INFORMED CONSENT

All the studies performed in human oocytes or embryos and described in this review article have been used after obtaining informed consents from the patients.

ORCID

Yasuyuki Mio https://orcid.org/0000-0002-0413-6728
Minori Nakaoka https://orcid.org/0000-0002-0385-4824
Panagiota Tsounapi https://orcid.org/0000-0002-6202-8653

REFERENCES

1. Payne D, Flaherty SP, Barry MF, Mathews CD. Preliminary observation on polar body extrusion and pronuclear formation in human oocytes using time-lapse video cinematography. Hum Reprod. 1997;12(3):532–41. https://doi.org/10.1093/humrep/12.3.532
2. Mio Y. Morphological analysis of human embryonic development using time-lapse cinematography. J Mamm Ova Res. 2006;23:27–36. https://doi.org/10.1274/jmor.23.27
3. Mio Y, Maeda K. Time-lapse cinematography of dynamic changes occurring during in vitro development of human embryos. Am J Obstet Gynecol. 2008;199(6):660.e1–660.e5. https://doi.org/10.1016/j.ajog.2008.07.023
4. Mio Y, Iwata K, Yumoto K, Maeda K. Human embryonic behavior observed with time-lapse cinematography. J Health Med Informat. 2014;5(1):143. https://doi.org/10.4172/2157-7420.1000143
5. Iwata K, Mio Y. Observation of human embryonic behavior in vitro by high-resolution time-lapse cinematography. Repro Med Biol. 2016;15(3):145–54. https://doi.org/10.1007/s12522-015-0231-7
6. Mio Y, Sekijima A, Iwabe T, Onohara Y, Harada T, Terakawa N. Subtle rise in serum progesterone during the follicular phase as a predictor of the outcome of in vitro fertilization. Fertil Steril. 1992;58(1):159–66. https://doi.org/10.1016/s0015-0282(16)55154-1
7. Veeck LL. Preembryo grading and degree of cytoplasmic fragmentation. An atlas of human gametes and conceptuses: an illustrated

reference for assisted reproductive technology. New York, London: The Parthenon Publishing Group; 1999. p. 46–51.
8. Alpha Scientists in Reproductive Medicine and ESHRE Special Interest Group of Embryology. The Istanbul consensus workshop on embryo assessment: proceedings of an expert meeting. Hum Reprod. 2011;26(6):1270–83. https://doi.org/10.1093/humrep/der037
9. Van Steirteghem AC, Liu J, Joris H, Nagy Z, Janssenswillen C, Tournaye H, et al. Higher success rate by intracytoplasmic sperm injection than by subzonal insemination. Report of a second series of 300 consecutive treatment cycles. Hum Reprod. 1993;8(7):1055–60. https://doi.org/10.1093/oxfordjournals.humrep.a138191
10. Van Steirteghem AC, Nagy Z, Joris H, Liu J, Staessen C, Smitz J, et al. Higher fertilization and implantation rates after intracytoplasmic sperm injection. Hum Reprod. 1993;8(7):1061–6. https://doi.org/10.1093/oxfordjournals.humrep.a138192
11. Payne D, Flaherty SP, Jeffery R, Warnes GM, Matthews CD. Successful treatment of severe factor infertility in 100 consecutive cycles using intracytoplasmic sperm injection. Hum Reprod. 1994;9(11):2051–7. https://doi.org/10.1093/oxfordjournals.humrep.a138392
12. Yanagimachi R. Mammalian fertilization. In: Knobil E, Neil JD, editors. The physiology of reproduction. Volume 1. New York: Raven; 1988. p. 135–85.
13. Yamasaki H, Hirao Y. Appearance of the incorporation cone and extrusion of the second polar body in hamster. J Mamm Ova Res. 1999;16(1):43–9. https://doi.org/10.1274/jmor.16.43
14. Shalgi R, Phillips DM, Kraicer PF. Observation on the incorporation cone in the rat. Gamete Res. 1978;1(1):27–37. https://doi.org/10.1002/mrd.1120010106
15. Davies TJ, Gardner RL. The plane of first cleavage is not related to the distribution of sperm components in the mouse. Hum Reprod. 2002;17(9):2368–79. https://doi.org/10.1093/humrep/17.9.2368
16. Maro B, Johnson MH, Pickering SJ, Flach G. Changes in Actin distribution during fertilization of the mouse egg. J Embryol Exp Morphol. 1984;81(1):211–37. https://doi.org/10.1242/dev.81.1.211
17. Piotrowska K, Zernicka-Goetz M. Role for sperm in spatial patterning of the early mouse embryo. Nature. 2001;409(6819):517–21. https://doi.org/10.1038/35054069
18. Schatten G. The centrosome and its mode of inheritance: the reduction of the centrosome during gametogenesis and its restoration during fertilization. Dev Biol. 1994;165(2):299–335. https://doi.org/10.1006/dbio.1994.1256
19. Simerly C, Wu GJ, Zoran S, Ord T, Rawlins R, Jones J, et al. The paternal inheritance of the centrosome, the cell's microtubule-organizing center, in humans, and the implications for infertility. Nat Med. 1995;1(1):47–52. https://doi.org/10.1038/nm0195-47
20. Terada Y, Simerly CR, Hewitson L, Schatten G. Sperm aster formation and pronuclear decondensation during rabbit fertilization and development of a functional assay for human sperm. Biol Reprod. 2000;62(3):557–63. https://doi.org/10.1095/biolreprod62.3.557
21. Van Blerkom J, Davis P, Merriam J, Sinclair J. Nuclear and cytoplasmic dynamics of sperm penetration, pronuclear formation and microtubule organization during fertilization and early preimplantation development in the human. Hum Reprod Update. 1995;1(5):429–61. https://doi.org/10.1093/humupd/1.5.429
22. Van Blerkom J, Davis P, Alexander S. Differential mitochondrial distribution in human pronuclear embryos leads to disproportionate inheritance between blastomeres: relationship to microtubular organization, ATP content and competence. Hum Reprod. 2000;15(12):2621–33. https://doi.org/10.1093/humrep/15.12.2621
23. Ebner T, Moser M, Sommergruber M, Gaiswinkler U, Wiesinger R, Puchner M, et al. Presence, but not type or degree of extension, of a cytoplasmic halo has a significant influence on preimplantation development and implantation behaviour. Hum Reprod. 2003;18(11):2406–12. https://doi.org/10.1093/humrep/deg452
24. Ezoe K, Miki T, Okimura T, Uchiyama K, Yabuuchi A, Kobayashi T, et al. Characteristics of the cytoplasmic halo during fertilization correlate with the live birth rate after fresh cleaved embryo transfer on day 2 in minimal ovarian stimulation cycles: a retrospective observational study. Reprod Biol Endocrinol. 2021;19(1):172. https://doi.org/10.1186/s12958-021-00859-1
25. Tesarik J, Kopency V. Assembly of the nucleolar precursor bodies in human male pronuclei is correlated with an early RNA synthetic activity. Exp Cell Res. 1990;191(1):153–6. https://doi.org/10.1016/0014-4827(90)90050-k
26. Peterson T. Growth factors in the nucleolus? J Cell Biol. 1998;143(2):279–81. https://doi.org/10.1083/jcb.143.2.279
27. Kyogoku H, Kitajima TS, Miyano T. Nucleolus precursor body (NPB): a distinct structure in mammalian oocyte and zygotes. Nucleus. 2014;5(6):493–8. https://doi.org/10.4161/19491034.2014.990858
28. Fulka H, Aoki F. Nucleolus precursor bodies and ribosome biogenesis in early mammalian embryos: old theories and new discoveries. Biol Reprod. 2016;94(6):143. https://doi.org/10.1095/biolreprod.115.136093
29. Tesarik J, Greco E. The probability of abnormal preimplantation development can be predicted by a single static observation on pronuclear stage morphology. Hum Reprod. 1999;14(5):1318–23. https://doi.org/10.1093/humrep/14.5.1318
30. Scott L. Pronuclear scoring as a predictor of embryo development. Reprod Biomed Online. 2003;6(2):201–14. https://doi.org/10.1016/s1472-6483(10)61711-7
31. Nakaoka M, Yumoto K, Shimura T, Mio Y. Dynamic and cytological analyses of pronuclei and centrosome positions in relation to the first cleavage plane in human embryos. Hum Reprod. 2019;34(Suppl 1):i3–i4. https://doi.org/10.1093/humrep/34.Supplement_1.1
32. Penderson T. The Centriole Mystique. Trends Cell Biol. 2020;30(8):590–3. https://doi.org/10.1016/j.tcb.2020.05.001
33. Vasquez-Limeta A, Loncarek J. Human centrosome organization and function in interphase and mitosis. Semin Cell Dev Biol. 2021;117:30–41. https://doi.org/10.1016/j.semcdb.2021.03.020
34. Ducibella T, Albertini DF, Anderson E, Biggers JD. The preimplantation mammalian embryo: characterization of intercellular junctions and their appearance during development. Dev Biol. 1975;45(2):231–50. https://doi.org/10.1016/0012-1606(75)90063-9
35. Hurst PR, Jefferies K, Eckstein P, Wheeler AG. An ultrastructural study of preimplantation uterine embryos of the rhesus monkey. J Anat. 1978;126(Pt 1):209–20.
36. Reeve WJ. Cytoplasmic polarity develops at compaction in rat and mouse embryos. J Embryol Exp Morphol. 1981;62:351–67.
37. Pratt HP, Ziomek CA, Reeve WJ, Johnson MH. Compaction of the mouse embryo: an analysis of its components. J Embryol Exp Morphol. 1982;70:113–32.
38. Enders AC, Lantz KC, Schlafke S. The morula-blastocyst transition in two Old World primates: the baboon and rhesus monkey. J Med Primatol. 1990;19(8):725–47.
39. Fleming TP, Hay M, Javed Q, Citi S. Localization of tight junction protein cingulin is temporally and spatially regulated during early mouse development. Development. 1993;117(3):1135–44. https://doi.org/10.1242/dev.117.3.1135
40. Koyama H, Suzuki H, Yang X, Jiang S, Foote RH. Analysis of polarity of bovine and rabbit embryos by scanning electron microscopy. Biol Reprod. 1994;50(1):163–70. https://doi.org/10.1095/biolreprod50.1.163
41. Fleming TP, Ghassemifar MR, Sheth B. Junctional complexes in the early mammalian embryo. Semin Reprod Med. 2000;18(2):185–93. https://doi.org/10.1055/s-2000-12557
42. Burns KH, Matzuk MM. Preimplantation embryogenesis. In: Neill JD, editor. Knobil and Neill's physiology of reproduction. Volume

1. Third ed. New York: ELSEVIER Academic Press; 2006. p. 261–310.
43. Iwata K, Yumoto K, Sugishima M, Mizoguchi C, Kai Y, Iba Y, et al. Analysis of compaction initiation in human embryos by using time-lapse cinematography. J Assist Reprod Genet. 2014;31(4):421–6. https://doi.org/10.1007/s10815-014-0195-2
44. Swann K, Lai FA. The sperm phospholipase C-Z and Ca^{2+} signalling at fertilization in mammals. Biochem Soc Trans. 2016;44(1):267–72. https://doi.org/10.1042/BST20150221
45. Yamazaki K, Suzuki R, Hojo E, Kondo S, Kato Y, Kamioka K, et al. Trypsin-like hatching enzyme of mouse blastocysts: evidence for its participation in hatching process before zona shedding of embryos. Develop Growth Differ. 1994;36(2):149–54. https://doi.org/10.1111/j.1440-169X.1994.00149.x
46. Gonzales DS, Jones JM, Pinyopummintr T, Carnevale EM, Ginther OJ, Shapiro SS, et al. Trophectoderm projections: a potential means for locomotion, attachment and implantation of bovine, equine and human blastocysts. Hum Reprod. 1996;11(12):2739–45. https://doi.org/10.1093/oxfordjournals.humrep.a019201
47. Thomas M, Jain S, Kumar GP, Laloraya M. A programmed oxy-radical burst causes hatching of mouse blastocysts. J Cell Sci. 1997;110(Pt14):1597–602. https://doi.org/10.1242/jcs.110.14.1597
48. Cimadomo D, Marcontteo A, Trio S, Chiappetta V, Innocenti F, Albricci L, et al. Human blastocyst spontaneous collapse is associated with worse morphological quality and higher degeneration and aneuploidy rates: a comprehensive analysis standardized through artificial intelligence. Hum Reprod. 2022;37(10):2291–306. https://doi.org/10.1093/humrep/deac175
49. Bodri D, Sugimoto T, Yao Serna J, Kawachiya S, Kato R, Matsumoto T. Blastocyst collapse is not an independent predictor of reduced live birth: a time-lapse study. Fertil Steril. 2016;105(6):1476–83. e3. https://doi.org/10.1016/j.fertnstert.2016.02.014
50. Terada Y, Hasegawa H, Ugajin T, Murakami T, Yaegashi N, Okamura K. Microtubule organization during human parthenogenesis. Fertil Steril. 2009;91(4):1271–2. https://doi.org/10.1016/j.fertnstert.2008.05.051
51. Bos-Mikich A, Bressan FF, Ruggeri RR, Watanabe Y, Meirelles FV. Parthenogenesis and human assisted reproduction. Stem Cells Int. 2016;2016:1970843. https://doi.org/10.1155/2016/1970843
52. Staessen C, Janssenswillen C, Devroey P, Van Steirteghem AC. Cytogenetic and morphological observations of single pronucleated human oocytes after in-vitro fertilization. Hum Reprod. 1993;8(2):221–3. https://doi.org/10.1093/oxfordjournals.humrep.a138026
53. Kai Y, Moriwaki H, Yumoto K, Iwata K, Mio Y. Assessment of developmental potential of human single pronucleated zygotes derived from conventional in vitro fertilization. J Assist Reprod Genet. 2018;35(8):1377–84. https://doi.org/10.1007/s10815-018-1241-2
54. Gras L, Trounson AO. Pregnancy and birth resulting from transfer of a blastocyst observed to have one pronucleus at the time of examination for fertilization. Hum Reprod. 1999;14(7):1869–71. https://doi.org/10.1093/humrep/14.7.1869
55. Itoi F, Asano Y, Shimizu M, Honnma H, Murata Y. Birth of nine normal healthy babies following transfer of blastocysts derived from human single-pronucleate zygotes. J Assist Reprod Genet. 2015;32(9):1401–7. https://doi.org/10.1007/s10815-015-0518-y
56. Wang T, Si J, Wang B, Yin M, Yu W, Jin W, et al. Prediction of live birth in vitrified-warmed 1PN-derived blastocyst transfer: overall quality grade, ICM, TE, and expansion degree. Front Physiol. 2022;13:964360. https://doi.org/10.3389/fphys.2022.964360
57. Sadowy S, Tomkin G, Munné S, Ferrara-Congedo T, Cohen J. Impaired development of zygotes with uneven pronuclear size. Zygote. 1998;6(2):137–41. https://doi.org/10.1017/s0967199498000057
58. Kai Y, Iwata K, Iba Y, Mio Y. Diagnosis of abnormal human fertilization status based on pronuclear origin and/or centrosome number. J Assist Reprod Genet. 2015;32(11):1589–95. https://doi.org/10.1007/s10815-015-0568-1
59. Mio Y, Iwata K, Yumoto K, Kai Y, Sargant HC, Mizoguchi C, et al. Possible mechanism of polyspermy block in human oocytes observed by time-lapse cinematography. J Assist Reprod Genet. 2012;29(9):951–6. https://doi.org/10.1007/s10815-012-9815-x
60. Saunders CM, Larman MG, Parrington J, Cox LJ, Royse J, Blayney LM, et al. PLC zeta: a sperm-specific trigger of Ca (2+) oscillations in eggs and embryo development. Development. 2002;129(15):3533–44. https://doi.org/10.1242/dev./129.15.3533
61. Saunders CM, Swann K, Lai FA. PLC zeta, a sperm-specific PLC and its potential role in fertilization. Biochem Soc Symp. 2007;74:23–36. https://doi.org/10.1042/BSS0740023
62. Wang Q, Racowsky C, Deng M. Mechanism of the chromosome-induced polar body extrusion in mouse eggs. Cell Div. 2011;6:17. https://doi.org/10.1186/1747-1028-6-17
63. Rubio I, Kuhlmann R, Agerholm I, Kirk J, Herrero J, Escribá MJ, et al. Limited implantation success of direct-cleaved human zygotes: a time-lapse study. Fertil Steril. 2012;98(6):1458–63. https://doi.org/10.1016/j.fertnstert.2012.1135
64. Fan YL, Han SB, Wu LH, Wang YP, Huang GN. Abnormally cleaving embryos are able to produce live births: a time-lapse study. J Assist Reprod Genet. 2016;33(3):379–85. https://doi.org/10.1007/s10815-015-0632-x
65. Desai N, Goldberg JM, Austin C, Falcone T. Are cleavage anomalies, multinucleation, or specific cell cycle kinetics observed with time-lapse imaging predictive of embryo developmental capacity or ploidy? Fertil Steril. 2018;109(4):665–74. https://doi.org/10.1016/j.fertstert.2017.12.025
66. Alikani M, Cohen J, Tomkin G, Garrisi GJ, Mack C, Scott RT. Human embryo fragmentation in vitro and its implications for pregnancy and implantation. Fertil Steril. 1999;71(5):836–42.
67. Payne D, Takeshita C, Wakatsuki Y, Iwata K, Kato Y, Ueno Y, et al. Fragmentation and cytokinesis in early human embryos. Hum Reprod. 2005;20(suppl 1):i13. https://doi.org/10.1093/oxfordjournals.humrep.a002353
68. Derrick R, Hickman C, Oliana O, Wilkinson T, Gwinnett D, Whyte LB, et al. Perivitelline threads associated with fragments in human cleavage stage embryos observed through time-lapse microscopy. Reprod Biomed Online. 2017;35(6):640–5. https://doi.org/10.1016/j.rmbo.2017.08.026
69. Kellam L, Pastorelli LM, Bastida AM, Senkbeil A, Montgomery S, Fishel S, et al. Perivitelline threads in cleavage-stage human embryos: observations using time-lapse imaging. Reprod Biomed Online. 2017;35(6):646–56. https://doi.org/10.1016/j.rbmo.2017.09.004
70. Gilchrist RB, Lane M, Thompson JG. Oocyte-secreted factors: regulators of cumulus cell function and oocyte quality. Hum Reprod Update. 2008;14(2):159–77. https://doi.org/10.1093/humupd/dmm040
71. Yumoto K, Shimura T, Mio Y. Removing the zona pellucida can decrease cytoplasmic fragmentations in human embryos: a pilot study using 3PN embryos and time-laspe cinematography. J Assist Reprod Genet. 2020;37(6):1349–54. https://doi.org/10.1007/s10815-020-01773-y
72. da Costa ALE, Abdelmassih S, de Oliveira FG, Abdelmassih V, Abdelmassih R, Nagy ZP, et al. Monozygotic twins and transfer at the blastocyst stage after ICSI. Hum Reprod. 2001;16(2):333–6. https://doi.org/10.1093/humrep/16.2.333
73. Aston KI, Peterson CM, Carrell DT. Monozygotic twinning associated with assisted reproductive technologies: a review. Reproduction. 2008;136(4):377–86. https://doi.org/10.1530/REP-08-0206

74. Vitthala S, Gelbaya TA, Brinson DR, Fitzgerald CT, Nardo LG. The risk of monozygotic twins after assisted reproductive technology: a systematic review and meta-analysis. Hum Rerod Update. 2009;15(1):45–55. https://doi.org/10.1093/humupd/dmn045
75. Dirvanauskas D, Maskeliunas R, Raudonis V, Damasevicius R. Embryo development stage prediction algorithm for automated time lapse incubators. Comput Methods Prog Biomed. 2019;177:161–74. https://doi.org/10.1016/j.cmpb.2019.05.027
76. Kragh MF, Karstoft H. Embryo selection with artificial intelligence: how to evaluate and compare methods? J Assist Reprod Genet. 2021;38(7):1675–89. https://doi.org/10.1007/s10815-021-02254-6
77. Dimitriadis I, Zaninovic N, Chavez Badiola A, Bormann CL. Artificial intelligence in the embryology laboratory: a review. Reprod Biomed. 2022;44(3):435–48. https://doi.org/10.1916/j.rbmo.2021.11.0031472-6483

SUPPORTING INFORMATION

Additional supporting information can be found online in the Supporting Information section at the end of this article.

How to cite this article: Mio Y, Yumoto K, Sugishima M, Nakaoka M, Shimura T, Tsounapi P. Morphokinetic features in human embryos: Analysis by our original high-resolution time-lapse cinematography—Summary of the past two decades. Reprod Med Biol. 2024;23:e12578. https://doi.org/10.1002/rmb2.12578